A New Apparatus for Brain Imaging: Four-Head Rotating Gamma Camera Single-Photon Emission Computed Tomograph

Kazufumi Kimura, Kazuo Hashikawa, Hideki Etani, Akira Uehara, Takahiro Kozuka, Hiroshi Moriwaki, Yoshinari Isaka, Masayasu Matsumoto, Takenobu Kamada, Hiromi Moriyama, and Hideho Tabuchi

Department of Nuclear Medicine, Biomedical Research Center, The First Department of Internal Medicine, Osaka University Medical School, National Osaka-minami Hospital, Osaka, Japan, and Hitachi Medical Corporation, Tiba, Japan

The development of a new rotating gamma camera SPECT device for imaging the brain was undertaken with the objective of achieving the highest full volume imaging spatial and temporal resolution performance. For this purpose, four rectangular gamma camera detectors were arranged as close to the head as possible, and united in a block to insure detector head registration and alignment as well as to enable rotation stability at high speeds. Phantom and clinical studies performed demonstrated 42 sequential, 4-mm thick transaxial images acquired in one scan and with sufficient volume to permit the entire cerebrum and cerebellum to be imaged with high sensitivity. The central field of view reconstructed spatial resolution measured 7.0 mm full width of half maximum utilizing the high-resolution collimator, and tomographic images of arbitrary planes including sagittal and coronal demonstrated equally high resolution. The high sensitivity and high speed rotational acquisition capability of the device permits dynamic SPECT studies to be carried out in the analysis of rapidly varying radiotracer concentrations.

J Nucl Med 1990; 31:603–609

Over the past several years, single-photon emission computed tomograph devices (SPECTs) have been developed at many institutes. Of those specifically developed for brain imaging, ring-type SPECTs have been designed to accomplish high resolution with high sensitivity (*1–7*). These systems typically acquire a limited set of slices at one time, and the longitudinal spatial resolution they achieve is inferior to their higher transaxial spatial resolution performance. We determined that, given the complex nature of the brain, the ability to acquire sequential images of the entire brain volume would be an essential component of a device intended to investigate brain metabolism and blood flow both in physiologic and pathologic conditions. For this purpose, we utilized a system of rotating gamma camera detectors which offer full volume imaging with near equivalence in reconstructed and transaxial resolution performance. While rotating gamma camera SPECT typically presents compromises in sensitivity and absolute spatial resolution when compared to ring-type SPECT, the result of our study and design was the successful development of a new rotating gamma camera SPECT with high sensitivity and resolution. A part of the present investigation has been reported in abstract form (*8*).

Received Feb. 6, 1989; revision accepted Dec. 7, 1989.

For reprints contact: Kazufumi Kimura, MD, Department of Nuclear Medicine, Biomedical Research Center, Osaka University Medical School, 1-1-50, Fukushima, Fukushima-ku, Osaka 553, Japan.

SYSTEM DESIGN

Detectors

Figure 1 shows the block diagram of our new four-head rotating gamma camera SPECT device (4-head SPECT). The four detectors, cubically blocked and registered to each other, rotate as a single unit arranged to surround a patient's head. Each matched detector consists of a collimator, a scintillation crystal (NaI(Tl), 26.0 cm × 20.8 cm × 9.0 mm), 30 photomultiplier tubes (PMTs), and preamplifiers. The scintillation crystal is a planar light guide coupled to a 6 × 5 array of PMTs. As depicted in Figure 2, special 2-in. square bialkali PMTs were utilized to permit construction of a dimensionally compact detector as compared to one having the same effective field of view (FOV) utilizing standard circular PMTs. The inactive perimetrical region at the edge of the detector (dead space) is only 7.0 cm, enabling optimization of camera/brain proximity and brain viewing volume including cerebellum without obstruction by the patient's shoulders.

Collimators

Four sets of matched collimators were designed to provide for low-energy high resolution (LEHR), low-energy general purpose (LEGP), low-energy high sensitivity (LEHS), and medium-energy general-purpose (MEGP) imaging. The low-energy collimators, suitable for Xenon-133, technetium-99m, and iodine-123 (p,5n) were designed for radioisotopes with no more than 170 keV with <1.2% septal penetration fractions. The MEGP, designed for up to 245 keV, permits acquisition of the two peaks of indium-111 as well as (p,2n) prepared ^{123}I radiolabels.

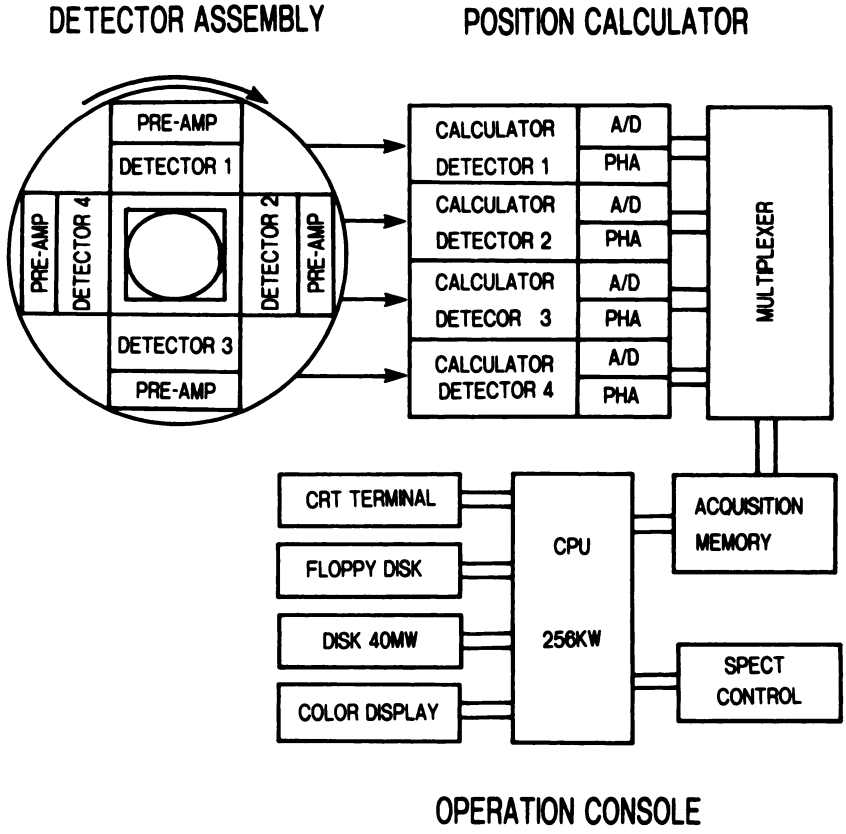

FIGURE 1
Block diagram of the 4-head SPECT, consisting of a detector assembly, position calculator and operation console units. The detector assembly incorporates four compact rectangular gamma camera detectors. A/D = analog to digital converter; PHA = pulse height analyzer.

While the same type of collimator is typically mounted on the four detectors, our design makes it possible to use different collimators for each detector and permits discrete data acquisition from each detector.

The Cerebral Aperture

The distance between the crystal surfaces of opposed rectangular detectors is 340 mm and as shown in Figure 3 defines an effective 220 mm axial × 170 mm longitudinal field of view for each detector. To accommodate patient positioning, our system incorporates a tri-point gallium arsenide laser projector, motorized table, and articulating head holder. The patient position can be set outside of the tunnel, after which alignment for imaging within the FOV is automatically affected by the system. While the orbitomeatal line is often used as the standard reference plane, provision of "free angle tomographic reconstruction" software in our system permits reorientation of the final tomographic images to any plane and correction of data acquired from mispositioned patients.

Electronics

As shown in Figure 1, application of a four-channel position calculation circuit permits discrete data to be acquired by each of the four detectors through a multiplexer into a 4 MW (8 MB) memory. In the position calculation circuit, positional data are digitally corrected to improve spatial linearity and regional energy sensitivity and uniformity. A 16-bit Mini-Computer central processing unit (CPU) equipped with a 256-kW (512 kB) memory was used to control the gantry motions and detectors, perform reconstruction, and process the data for analysis and display. A 64-bit image processor is also incorporated to provide minimal processing time.

Data Acquisition

Two modes of detector head rotation were incorporated in our design; angular stepping and continuous sweeping orbits. To accomplish simultaneous four-view and standard "static SPECT" acquisitions, a stepped-angle rotation mode is selected. SPECT data acquired from rotations of 90, 180, and 360 degrees can be reconstructed, and the number of angular sampling (azimuth) possible per revolution, is 32, 64, or 128. An acquisition time per step is selectable from 1 to 99 sec sampling, while the continuous mode utilized for temporal/dynamic SPECT studies provides rotation speeds of 10, 20, 40, or 80 sec/360° rotation. These stable high rotation speeds enable dynamic SPECT imaging useful in evaluating radionuclide kinetics.

Acquisition matrixes including 32×32, 64×64, and 128×128 were provided, of which the 64×64 matrix represents a 4-mm × 4-mm/pixel area and 42 sequential images of 4-mm thick transaxial slices to be obtained simultaneously. During acquisition, on-the-fly uniformity, linearity, and energy corrections are affected by each digital processor for each gamma camera detector channel.

PERFORMANCE CHARACTERISTICS

Table 1 characterizes the performance results of our 4-head SPECT according to NEMA standard tests (*9*). The spatial resolution of a ^{99m}Tc line source, in scatter 10 cm from the surface of the LEHR collimator, measured 6.9 mm FWHM with a reconstructed system spatial resolution of 7.0 mm FWHM at central field of view (CFOV). The highest sensitivity for our system

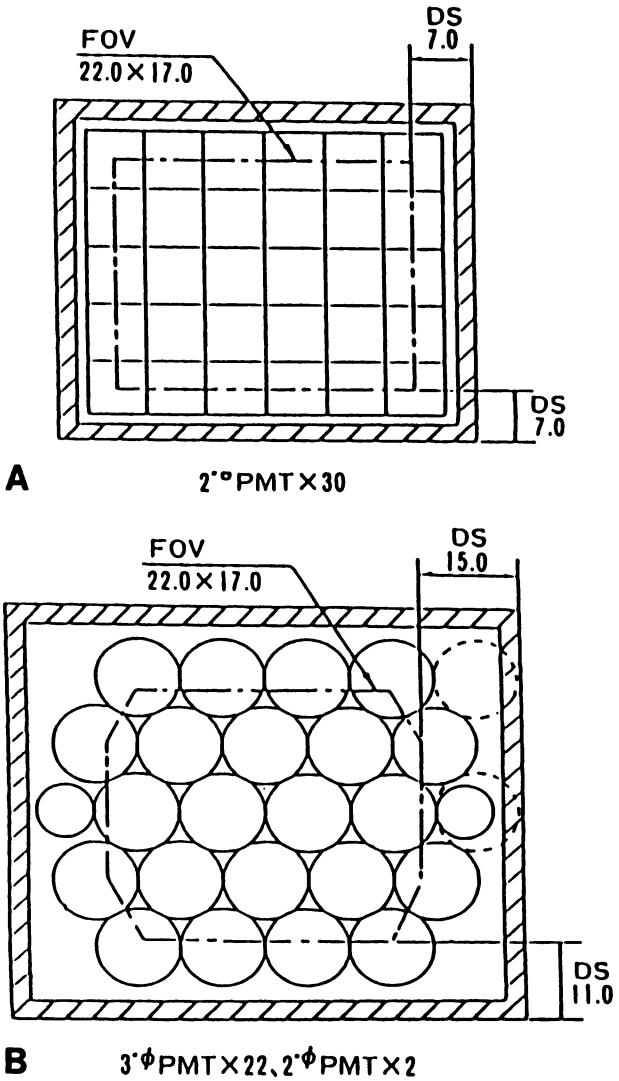

FIGURE 2
Schematic drawings comparing the 4-head SPECT detector (A) with that of a detector assembled utilizing standard 3-in. circular PMTs (B). Use of 2-in. square-shaped PMTs (A) permitted maintenance of the FOV and reduction of peripheral dead spaces as compared to use of standard PMTs (7.0 vs. 15.0 or 11.0 cm). DS = dead space; FOV = field of view; PMT = photo-multiplier tube.

was achieved with the LEHS collimator with a measurement of 1,240 cpm/37 kBq. Figure 4 demonstrates the reconstructed image resolution of a Hoffman brain phantom with our device as compared to that produced by a x-ray CT scanner. Discrimination of the detailed structures of the phantom are possible with the 4-head SPECT device described.

PRELIMINARY CLINICAL APPLICATIONS

Clinical utility of our 4-head SPECT device was investigated with application to patients with ischemic cerebrovascular diseases. As shown in Figure 5, in the unaffected areas of the brain, several brain structures such as the cerebral cortex, the thalamus, the putamen, the caudate nucleus and the cerebellar cortex are clearly discriminated as high-activity areas. Additionally, the three-dimensionality of the lesions shown are easily understood as low-activity areas in the serial transaxial, sagittal, and coronal images obtained with ^{99m}Tc-hexamethylpropyleneamine oxime (HMPAO). In another patient with hemianopsia (Figure 6), abnormalities in the cerebral blood flow (CBF) and the blood-brain barrier (BBB) are clearly demonstrated in the transaxial and sagittal SPECT images obtained with ^{123}I-isopropyl-p-iodoamphetamine (IMP) and ^{99m}Tc-DTPA, respectively.

DISCUSSION

To accomplish high resolution and high sensitivity imaging of the brain, a number of SPECT devices and methods have been developed and reported (*1–7*). One early brain SPECT device utilizing an annular ring scintillation crystal initially incorporated single slice detector arrays (*4*), while later models acquire several slices by multiplying the ring detector arrays. Even those

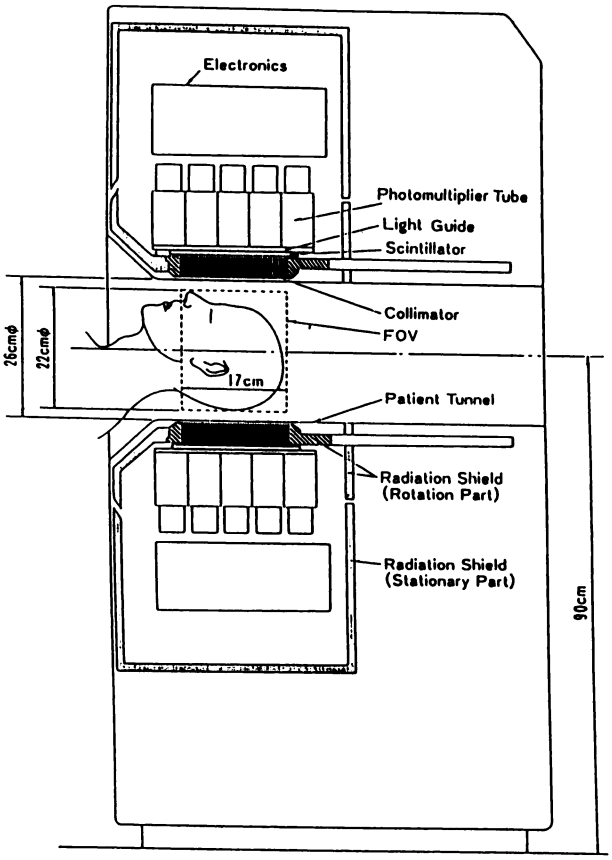

FIGURE 3
Cross section of the 4-head SPECT. The effective field of view (FOV) defines 220 mm (axial) by 170 mm (longitudinal) volume for imaging of the whole brain including cerebellum.

TABLE 1
Performance of Four-Head SPECT (NEMA Standard Test)

		CFOV	UFOV
1. Intrinsic spatial resolution			
	FWHM	3.0 mm	3.1 mm
	FWTM	5.8 mm	5.9 mm
2. Intrinsic flood field uniformity			
Integral uniformity		±3.0%	±4.0%
Differential uniformity		±2.0%	±2.7%
3. Intrinsic spatial linearity			
Absolute linearity		2.5 mm	2.5 mm
Differential linearity		0.7 mm	0.7 mm
4. Intrinsic count rate performance			
Maximum count rate (per one detector)		222.5 kcps	
5. System spatial resolution with scatter and sensitivity (per one detector)			

Collimator	FWHM	FWTM	Sensitivity
LEHR	6.9 mm	13.9 mm	101 cpm/37 kBq
LEGP	13.7 mm	29.1 mm	484 cpm/37 kBq
LEHS	24.2 mm	49.5 mm	1240 cpm/37 kBq
MEGP	13.2 mm	26.5 mm	350 cpm/37 kBq

6. Reconstructed system spatial resolution

Collimator	At center	Radial at 80 mm	Tangential at 80 mm
LEHR	7.0 mm	7.1 mm	6.2 mm
LEGP	13.0 mm	13.4 mm	8.9 mm
LEHS	21.3 mm	21.4 mm	13.8 mm
MEGP	14.6 mm	14.9 mm	9.2 mm

Source: ^{99m}Tc 1 mm diameter line source in air.
Acquisition: 128 × 128 matrix, 128 views.
Reconstruction filter: Ramachandran filter.
Pre-filter: Wiener filter.

CFOV = central field of view; UFOV = useful field of view; FWHM = full width of half maximum; FWTM = full width of tenth maximum; LEHR = low-energy high resolution collimator; LEGP = low-energy general-purpose collimator; LEHS = low-energy high sensitivity collimator; MEGP = middle-energy general purpose collimator.

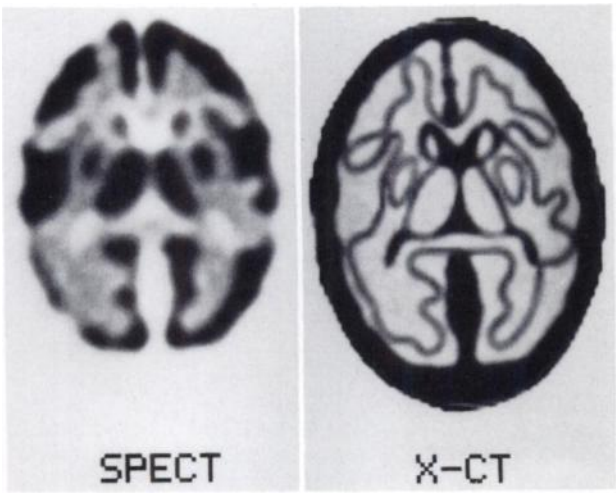

FIGURE 4
A 4-head SPECT image of the Hoffman brain phantom filled with ^{99m}Tc solution (left) next to a x-ray CT image of the same phantom (right). The high spatial performance of the 4-head SPECT permits visualization of the detailed structures within the phantom. Equipped with the LEHR collimator, approx 20,000,000 counts were collected over 128 steps into a 128 × 128 matrix (40 sec/step). Original data was pre-filtered with a 2-D Wiener filter prior to reconstruction with a Ramachandran (RAMP) filter, after which Chang's postreconstruction attenuation correction (*10*) was applied.

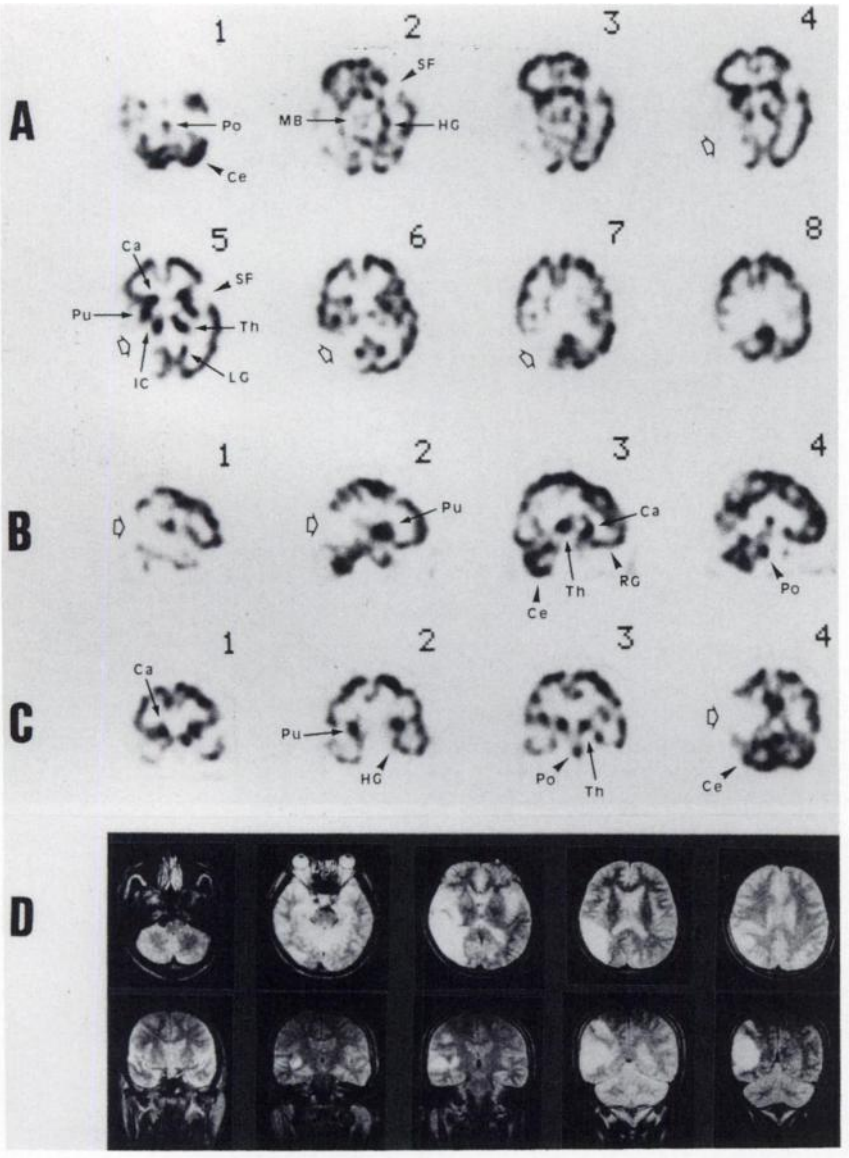

FIGURE 5
Technetium-99m-hexamethylpropyleneamine oxime (HMPAO) images (A, B, and C) and the T2-weighted MRI images (D) of a patient with cerebral infarction in the region of the middle cerebral artery. SPECT acquisition was performed 10 min after intravenous injection of 740 MBq ^{99m}Tc-HMPAO for 20 min, utilizing the LEHR collimator, 64 steps, and a 64 × 64 matrix. Approximately 6,300,000 total counts were acquired, and the original data was pre-filtered with a 2-D Wiener filter and then reconstructed with a Ramachandran backprojection filter. Chang's postreconstruction attenuation correction was applied to the transaxial data. A-C show the representative images of the transaxial, sagittal and coronal images respectively. The open arrows indicate the low CBF areas corresponding to the areas with infarction which are depicted in the MRI images (D). The four transaxial slices numbered 2 to 5 represent four sequential images obtained at a 4-mm thickness. Differences identified between two sequential images characterize excellent longitudinal resolution. Ca = caudate nucleus; Th = thalamus; Pu = putamen; IC = internal capsule; SF = sylvian fissure; MB = midbrain; RG = rectal gyrus; HG = hippocampal gyrus; Ce = cerebellum; Po = pons.

modified multi-slice ring-type SPECT devices are restricted volume imagers, and demonstrate inferior longitudinal resolution as compared to their higher transaxial resolution performance. In contrast, while some general-purpose single-head rotating gamma camera SPECT devices can acquire the entire brain volume simultaneously in one scan, the sensitivity and resolution achieved is inferior to ring-type SPECT. To overcome the disadvantage of single detector rotating gamma camera SPECT, multidetector gamma camera systems (*11,12*), slant collimators, and edge-cutting collimators and detectors (*13–16*) have been developed and applied commercially. Despite these efforts, improvements in sensitivity and resolution have not been satisfactory and the application of these devices and methods for dynamic SPECT study have been severely restricted or impossible. The approach taken with our 4-head SPECT device is similar in concept to the MARK IV system developed by Kuhl and colleagues (*1*), although their device was not based on gamma camera detectors. Our design objective targeted achieving three-dimensional volume imaging with high sensitivity, equivalent high resolution in all planes, and sufficient temporal resolution to permit dynamic SPECT applications. To achieve these goals, priority was given to the development of higher performance detectors with optimized positional proximity to the head, maximization of viewing volume and data collection sensitivity, and high speed multiple rotation stability for detector orbit motions. Four compact rectangular detectors were developed utilizing newly designed 2-in. square-shaped bialkali PMTs. Our design, utilizing these PMTs, permitted improved intrinsic resolution performance (Table 1) with minimization of the detector's inactive "detector edge to FOV" peripheral area (Figure 2). The detectors, small enough to be positioned

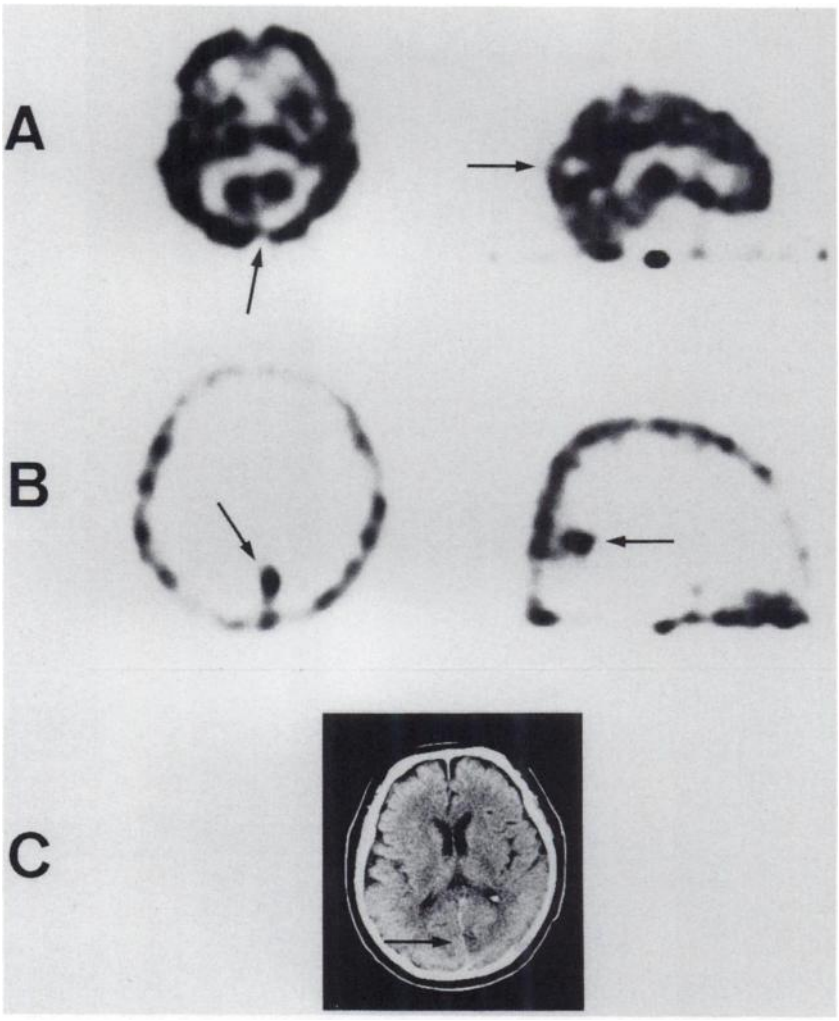

FIGURE 6
The ^{123}I-IMP SPECT images (A), ^{99m}Tc-DTPA SPECT images (B), and a x-ray CT image (C) of a patient with hemianopsia due to cerebral infarction. The transaxial (left) and sagittal (right) ^{123}I-IMP images (A), which were obtained 12 days after onset of symptoms, clearly shows the perfusion defect in the right visual cortex. A x-ray CT image obtained 30 days after onset defined a low density area in the same area. Transaxial (left) and sagittal (right) ^{99m}Tc-DTPA images (B) at 20 days after onset also clearly demonstrates the abnormal accumulation reflecting disruption in the blood-brain barrier in the same area in which the IMP images depict a perfusion defect. SPECT acquisition of ^{123}I-IMP image was performed 10 min after the i.v. injection of 222 MBq ^{123}I-IMP for 35 min, 64 steps, utilizing the LEHR collimator into a 64 × 64 matrix for approx 6.5 million counts. The original data was prefiltered using 2-D Wiener filter, backprojected with a Ramachandran filter, and corrected for attenuation by Chang's 1st order method. SPECT acquisition of the ^{99m}Tc-DTPA image was performed 10 min after i.v. injection of 740 MBq ^{99m}Tc-DTPA for 28 min, 64 steps, into a 64 × 64 matrix. Three million total counts were acquired, and images were processed identically to the IMP set using the attenuation data for ^{99m}Tc.

close to the head without obstruction by the patient's shoulders, allow full volume imaging of the cerebellum in the FOV (Figure 3). In a multidetector SPECT system, a small distortion of the detector alignment in the rotation results in marked reduction of spatial resolution and uniformity in the reconstructed images. In order to minimize this distortion, our application of multiple detectors were cubically mounted and rotated as a single block. The block of detectors can rotate at 6 rpm with stability, permitting 10-sec clockwise/counter-clockwise continuous revolutions used for temporal resolution dynamic SPECT studies. Furthermore, continuous rotation at high speeds and the integration of counts for each detector position into discrete memories permits the actual coincident events over 360° to be registered, as the time delay between acquisitions from each direction is not >2.5 sec. This function enabled us to eliminate artifacts caused by activity variations (*17*) and to obtain high quality images in static studies accomplished with rapidly varying radiotracer concentrations.

Tomographic reconstructed spatial resolution utilizing our device equipped with the LEHR collimator demonstrated 7.0 mm FWHM at the center with a longitudinal spatial resolution of 6.9 mm FWHM. To achieve 4.0-mm thick slices, 42 sequential transaxial images were obtained covering the entire brain volume. A maximum system sensitivity of 1,240 cpm/37 kBq was documented with ^{99m}Tc utilizing the LEHS collimator, approximately ten times higher than measurements obtained with a single-head SPECT camera and a similar collimator (*3*). Preliminary clinical application of our device has clearly demonstrated the potential usefulness of imaging detailed brain structures and precise visualization of the three-dimensional extent of lesions present.

ACKNOWLEDGMENTS

The authors thank Mr. Takatoshi Marumaya, Mr. Yukio Nakamura and Mr. Yoshimi Kusumi for their excellent technical assistance, Miss Yoko Yoshikawa, Miss Hiromi Taku and Miss Kuniyo Kawanishi for their secretarial assistance, and Mr. Gary Enos for his editorial and compositional assistance.

This work was supported in part by Smoking Research Foundation.

REFERENCES

1. Kuhl DE, Edwards RQ, Ricci AR, et al. The Mark IV system for radionuclide computed tomography of the brain. *Radiology* 1976; 121:405–413.
2. Rogers WL, Cinthorne NH, Stamos J, et al. SPRINT: A single photon ring tomograph [Abstact]. *J Nucl Med* 1982; 23:59.
3. Budinger TF. Revival of clinical nuclear medicine brain imaging. *J Nucl Med* 1981; 22:1094–1097.
4. Kanno I, Uemura K, Miura S, et al. HEADTOME: a hybride emission tomography for single photon and positron emission imaging of the brain. *J Comp Assist Tomogr* 1981; 5:216–226.
5. Hirose Y, Ikeda Y, Higashi Y, et al. A hybrid emission CT-HEADTOME. *IEEE Trans Nucl Sci* 1982; NS-29:520–523.
6. Lassen NA, Sveinsdottir E, Kanno I, et al. A fast moving, single photon emission tomograph for regional cerebral blood flow studies in man [Abstract]. *J Comp Assist Tomogr* 1978; 2:661–662.
7. Stokely EM, Sveinsdottir E, Lassen NA, et al. A single-photon dynamic computer assisted tomography (DCAT) for imaging brain function in multiple cross section. *J Comp Assist Tomogr* 1980; 4:230–240.
8. Hashikawa K, Kimura K, Isaka Y, et al. A new apparatus for brain imaging: four-head rotating gamma camera spect. *J Cereb Blood Flow Metab* 1989; 9(suppl 1):s736.
9. National Electric Manufacturers Association. NEMA standards publication for performance measurements of scintillation cameras. (No. NUI-1980), Washington, 1980.
10. Chang LT. A method for attenuation correction in radionuclide computed tomography. *IEEE Trans Nucl Sci* 1979; NS-26:2780–2789.
11. Jaszczak RJ, Chang LT, Stein NA, et al. Whole-body single photon emission computed tomography using dual, large-field-of-view scintillation cameras. *Phys Med Biol* 1986; 24:1184–1191.
12. Lim Y, Gottschalk S, Walker R, et al. Triangular SPECT system for 3-D total organ volume imaging: design concept and preliminary results. *IEEE Trans Nucl Sci* 1985; NS-32:741–747.
13. Larsson SA, Bergstrand G, Bergstedt H, et al. A special cut-off gamma camera for high-resolution SPECT of the head. *J Nucl Med* 1984; 25:1023–1030.
14. Peter DE, Philip OA, Robin JM, et al. Angled-collimator SPECT (A-SPECT): an improved approach to cranial single photon emission tomography. *J Nucl Med* 1984; 25:805–809.
15. Larsson SA, Bergstrand G, Bergstedt HF, et al. A specially cut-off gamma camera for high spatial resolution SPECT of the head. *J Nucl Med* 1984; 25:1023–1030.
16. Polak JF, Holman BL, Moretti JL, et al. I-123 HIPDM brain imaging using a rotating gamma camera equipped with a slant-hole collimator. *J Nucl Med* 1984; 25:495–498.
17. Bok BD, Bice AN, Clausen M, et al. Artifacts in camera-based single photon emission tomography due to activity variation. *Eur J Nucl Med* 1987; 13:439–442.